

## Research on a New Miniaturization Method of Patch Antenna Based on Metal Strip

Yanwen Hu<sup>1,\*</sup>, Shoudong Li<sup>1</sup>, Tingrong Zhang<sup>1</sup>, Wenying Zhou<sup>2</sup>, and Xiufang Wang<sup>3</sup>

**Abstract**—A new miniaturized patch antenna based on a metal strip is proposed in this paper. The antenna is designed by adding a middle metal strip layer to the substrate of a traditional rectangular patch antenna. By increasing the length of the metal strip, the working frequency of the patch antenna can be continuously reduced without significantly impacting the radiation pattern. The simulation results indicate that as the metal strip length increases from 5 mm to 25 mm, the working frequency of the patch antenna decreases from 2.39 GHz to 1.84 GHz, and its gain decreases from 6.72 dBi to 5.4 dBi. Two antenna samples with metal strip lengths of 5 mm and 20 mm are fabricated. The experimental results indicate that their working frequencies are 2.64 GHz and 2.43 GHz, respectively. And the radiation patterns of two antennas are consistent with the simulated results. All results confirm the effectiveness of the proposed miniaturization method.

### 1. INTRODUCTION

With the continuous development of the wireless communication technology, 5G technology has been widely used in communication systems, and 6G technology is also under development. To enhance the channel capacity and solve the problem of huge data volume without changing the frequency resources, researchers proposed multiple-input multiple-output (MIMO) communication technology. Therefore, MIMO antenna design has become the current research focus. Compared with single antennas, MIMO antennas can not only effectively suppress the multipath fading effect, improve signal reliability and stability, but also efficiently transmit more signals without expanding the signal bandwidth. Although MIMO antennas have incomparable advantages over single antennas, they also have some inherent defects. For instance, the geometric dimensions of MIMO antennas are much larger than that of single antennas, and the strong mutual coupling between multiple antenna elements is inevitable. As integration levels in modern electronic communication equipment continue to increase, the space volume available for antennas is diminishing. Therefore, the miniaturization research of MIMO antennas has important academic significance and engineering implication values.

Reducing the size of individual antennas is critical for designing compact MIMO antennas. The miniaturization technologies proposed by researchers mainly include: bending and meandering current technology [1], loading short line or short circuit pin technology [2,3], loading capacitive branch technology [4], etching defect ground technology [5], slotting on radiation patch technology [6], fractal technology [7,8], loading lumped elements technology [9], loading metamaterials technology [10,11], etc. In [12], a dual-band miniaturized antenna designed by using a fractal metamaterial structure is introduced. The antenna works at 4.4 GHz and 6.1 GHz and has a compact section size of  $20 \times 20 \text{ mm}^2$ . In [13], a corrugated miniaturized microstrip patch antenna designed by using a slotting

---

*Received 29 March 2023, Accepted 8 June 2023, Scheduled 17 June 2023*

\* Corresponding author: Yanwen Hu (2622898791@qq.com).

<sup>1</sup> School of Automation and Electrical Engineering, Lanzhou Jiaotong University, Lanzhou, China. <sup>2</sup> Key Lab of Opto-Electronic Technology and Intelligent Control of Ministry of Education, Lanzhou Jiaotong University, Lanzhou, China. <sup>3</sup> School of Physical Science and Technology, Southwest Jiaotong University, Chengdu, China.

technique on the radiation patch is proposed. The antenna works at 9 GHz and has a small size of  $0.16\lambda \times 0.16\lambda \times 0.04\lambda$ . In [14], a miniaturized microstrip patch antenna with a U-shaped slot on the radiation patch is mentioned. Its bandwidth is 167.6 MHz, which is slightly wider than that of the original antenna. In [15], a novel miniaturized microstrip patch antenna designed by curving the patch edges is introduced. Ultimately, the physical size of the designed antenna is reduced to 63.5% of the typical patch antenna. In [16], a miniaturized circular patch antenna loaded with a helical coil with magnetic negative characteristics is presented. The authors designed and fabricated two antennas with different parameters, and they demonstrated a size reduction of 40% and 60%, respectively. In [17], a miniaturized microstrip patch antenna designed by using a magnetic metamaterial substrate is proposed. This design achieves a size reduction of approximately 65% compared to traditional microstrip antennas, while maintaining almost unchanged bandwidth. In [18], a miniaturized high-gain microstrip patch antenna designed by combining a magnetic metamaterial substrate and a metamaterial coating is discussed. The antenna's size is  $170 \times 170 \times 37 \text{ mm}^3$ , which is less than  $\lambda/100$ . In [19], a miniaturized magnetoelectric dipole antenna designed by loading a magnetic metamaterial is proposed. Compared with the original antenna, the size of the antenna is reduced by 48%. In [20], a miniaturized circular patch antenna is designed by adding a complementary resonant ring between the radiation patch and the ground plate. Although the miniaturization process results in a reduction of radiation efficiency and loss of bandwidth, the patch area is reduced by 1/16, and the antenna performance remains acceptable. In [21], a laminated miniaturized patch antenna designed by using resonant ring and magnetic material is proposed. The section size of this antenna is  $30 \times 30 \text{ mm}^2$ , which is 64% smaller than traditional antennas. In [22], a miniaturized broadband metasurface antenna designed by loading cross-layer capacitance is introduced. The proposed antenna has a size of  $0.41\lambda \times 0.41\lambda$  and a bandwidth of 44.4%. Although a large number of miniaturized antenna design methods have been mentioned, few studies have focused on continuously adjusting the antenna working frequency by only adjusting additional structural parameters without changing the original parameters. In addition, researchers have proposed a large number of decoupling strategies, such as adding decoupling network [23], electromagnetic bandgap structure [24], defective ground structure [25], neutral line [26], and lumped inductance [27]. Combining these methods with suitable antenna miniaturization techniques could potentially lead to further reduction in the overall size of MIMO antennas.

In this paper, a novel design method for miniaturized patch antennas based on metal strips is proposed. By adding a metal strip layer between the ground plate and radiation patch of the traditional patch antenna, the working frequency of the antenna can be continuously adjusted without changing its overall size. This approach realizes antenna miniaturization with a slight impact on the radiation pattern. Specifically, as the length of the metal strip increases, the working frequency of the antenna decreases correspondingly. This design method may be combined with decoupling techniques to further develop miniaturized MIMO antennas, such as the previous research achievements of our team, as described in [28].

## 2. ANTENNA STRUCTURE

The structure of the miniaturized patch antenna based on the metal strip designed in this paper is shown in Figure 1. The antenna consists of three metal layers (grounding plate, intermediate metal strip, and radiation patch) and two dielectric plates (Sub1 and Sub2). The thickness of the metal layer is 0.035 mm. The dielectric plates are made of RO4350B, with a relative permittivity of 3.48 and a tangent of dielectric loss angle of 0.004. The thicknesses of the two dielectric plates are 1.524 mm and 0.508 mm, respectively. Additional structural parameters are provided in Figure 1. It should be noted that  $l$  represents the length of the intermediate metal strip, and  $g$  represents the distance between the upper and lower dielectric plates.

The antenna design process can be divided into two steps. In the first step, according to the design formulas of the rectangular patch antenna, the antenna that can work near 2.45 GHz is designed and optimized. In the second step, the metal strip and air gap are added to the antenna, and its radiation pattern and working frequency variation are studied as the dimensions of the additional structure are modified. The initial structural parameters ( $W$  and  $L$ ) of the rectangular patch antenna can be

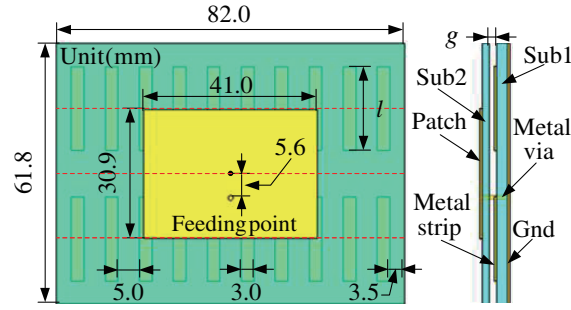


**Figure 1.** Structure model of the proposed antenna.

calculated from formulas (1)–(4).

$$W = \frac{c}{2f} \left( \frac{\varepsilon_r + 1}{2} \right)^{-\frac{1}{2}} \quad (1)$$

$$L = \frac{c}{f\sqrt{\varepsilon_e}} - 2\Delta L \quad (2)$$

$$\varepsilon_e = \frac{\varepsilon_r + 1}{2} + \frac{\varepsilon_r - 1}{2} \left( 1 + 12 \frac{h}{W} \right)^{-\frac{1}{2}} \quad (3)$$

$$\Delta L = 0.412h \frac{(\varepsilon_e + 0.3)(W/h + 0.264)}{(\varepsilon_e - 0.258)(W/h + 0.8)} \quad (4)$$

where  $c$  is the speed of light,  $f$  the working frequency,  $h$  the thickness of the dielectric plate,  $\varepsilon_r$  the relative permittivity,  $\varepsilon_e$  the equivalent relative permittivity, and  $\Delta L$  the length of the equivalent radiation gap.

Figure 2 shows the schematic diagram of the transmission line model of the antenna.  $Y_{in}$  is the input susceptance of the antenna;  $Y$  is the characteristic susceptance of the patch;  $L_1$  and  $L_2$  are the equivalent distance from the feeding point to the radiation slot;  $B_r$  is the capacitive susceptance of the radiation slot; and  $Y_r$  is the radiation susceptance. When the length of the metal strip changes,  $Y$ ,  $B_r$ , and  $Y_r$  will change accordingly, resulting in the change of the working frequency of the antenna.

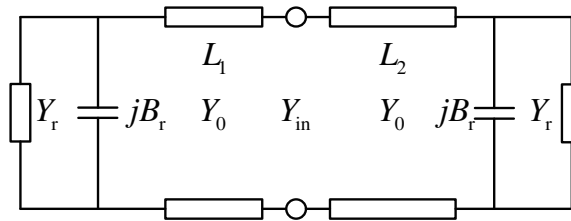


**Figure 2.** Transmission line model of the proposed antenna.

### 3. ANTENNA PERFORMANCE ANALYSIS

To illustrate the effectiveness of the miniaturization method, the performance of the proposed antenna is simulated and analyzed by using the numerical calculation method based on finite element method. The input impedance of the antenna is  $50 \Omega$ . The reflection coefficients  $S_{11}$  of the antenna under different values of  $l$  and  $g$  are simulated, and the simulation results are shown in Figure 3.

Figure 3(a) shows the simulation results of  $S_{11}$  at various values of  $l$  when  $g = 0$  mm, and the other parameters remain unchanged. It can be seen that the working frequency of the antenna without metal strip is 2.5 GHz. When  $l$  increases from 5 mm to 25 mm, the working frequency of the antenna

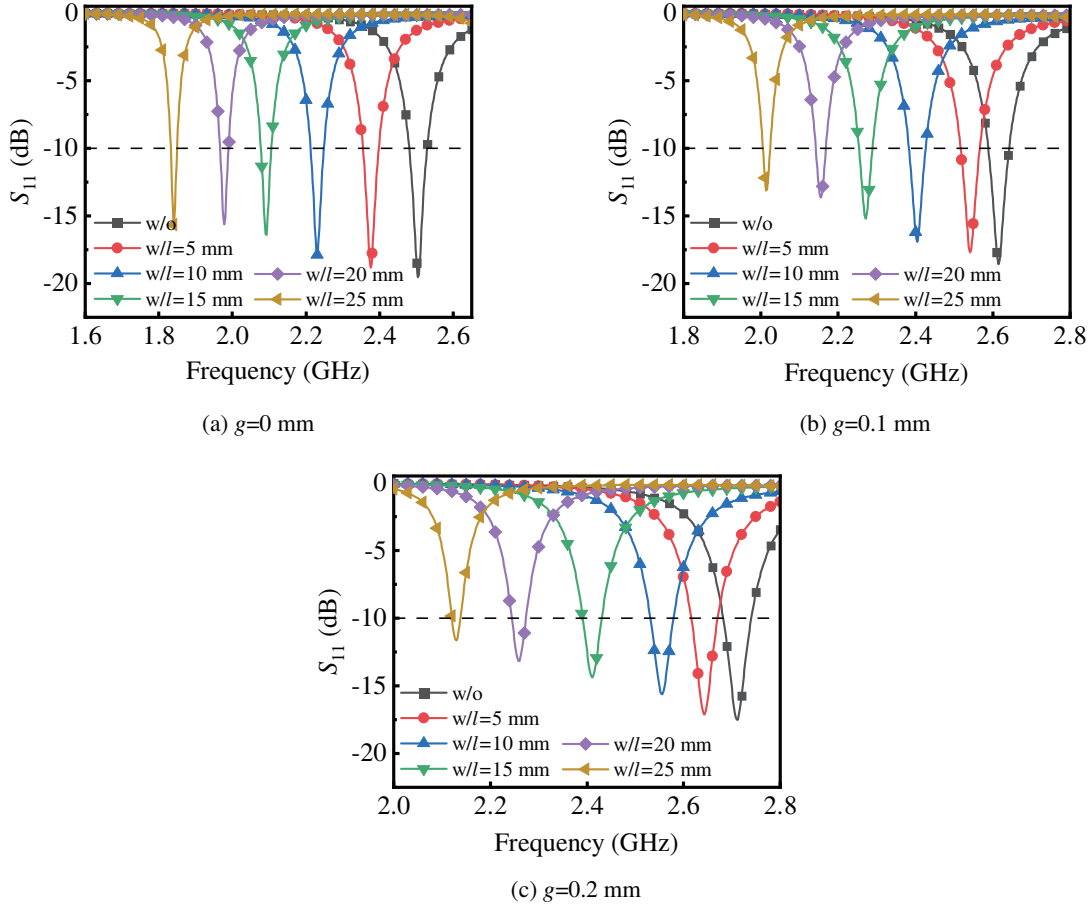


**Figure 3.** Simulation results of the antenna reflection coefficients under different structural parameters.

decreases from 2.39 GHz to 1.84 GHz. Figure 3(b) shows the simulation results of  $S_{11}$  at various values of  $l$  when  $g = 0.1$  mm and the other parameters remain unchanged. When  $l$  increases from 5 mm to 25 mm, the working frequency of the antenna decreases from 2.54 GHz to 2.02 GHz. Figure 3(c) shows the simulation results of reflection coefficients at various values of  $l$  when  $g = 0.2$  mm, and the other parameters remain unchanged. When  $l$  increases from 5 mm to 25 mm, the working frequency of the antenna decreases from 2.64 GHz to 2.15 GHz. The above results show the feasibility of the proposed method to reduce the antenna size.

For some antenna miniaturization methods, the radiation pattern of the antenna would be affected greatly after the antenna is miniaturized. Different from the traditional miniaturization methods, the radiation pattern of our proposed compact antenna is basically unaffected, and only its gain is slightly affected. Figure 4 shows the 3D radiation patterns of the antenna when  $l = 5$  mm and  $l = 20$  mm. It shows that the radiation patterns are consistent in all cases. When  $g = 0$  mm, the gains are 6.72 dBi and 5.95 dBi, respectively. When  $g = 0.1$  mm, the gains are 7.08 dBi and 6.55 dBi, respectively. When  $g = 0.2$  mm, the gains are 7.34 dBi and 6.89 dBi, respectively. The above research results reveal the advantages of our miniaturization method.

Figure 5 illustrates the variation curves of the antenna's working frequency and gain in relation to the length of  $l$ . The results demonstrate that as the length of  $l$  increases, both the working frequency and gain gradually decrease. When  $g = 0$  mm and  $l = 25$  mm, the gain of the antenna at the working frequency is 5.4 dBi. When  $g = 0.1$  mm and  $l = 25$  mm, the gain of the antenna at the working frequency is 6.24 dBi. When  $g = 0.2$  mm and  $l = 25$  mm, the gain of the antenna at the working frequency is 6.64 dBi, which is higher than the previous two cases.

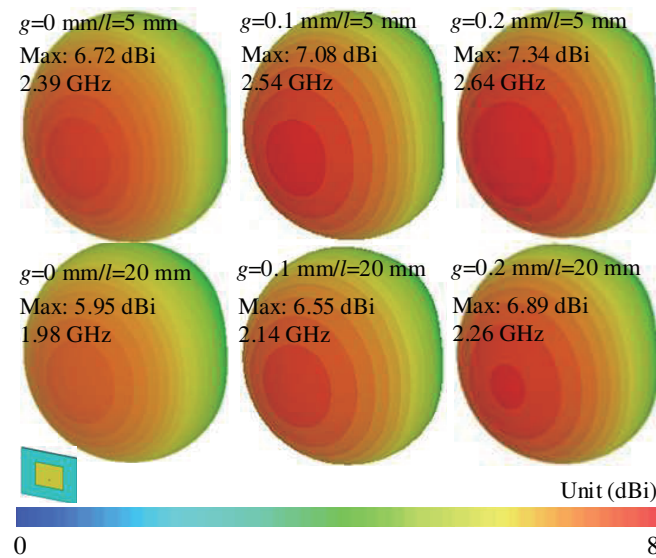


Figure 4. 3D radiation patterns of the proposed antenna.

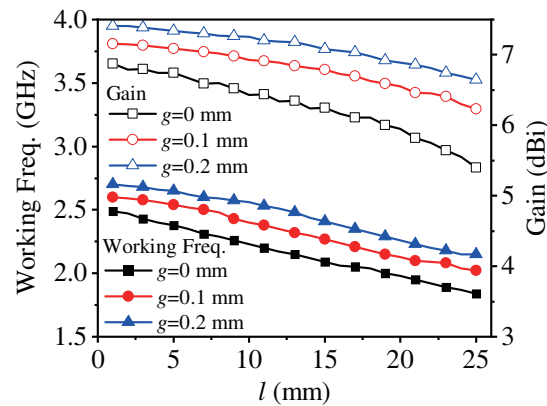


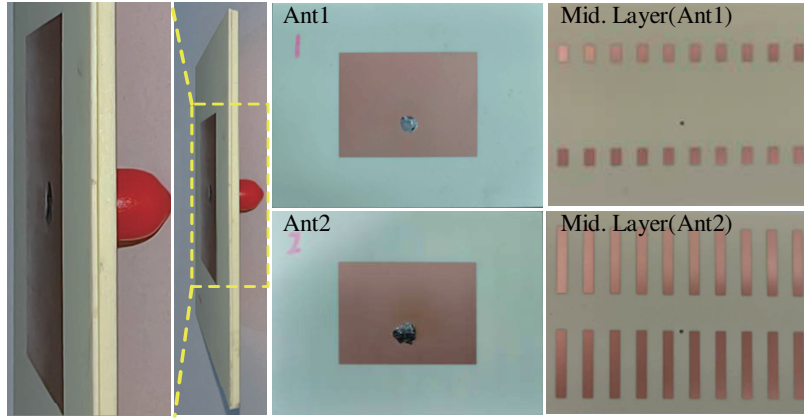
Figure 5. Variation curves of antenna's working frequency and gain with different  $l$ .

#### 4. EXPERIMENTAL MEASUREMENT

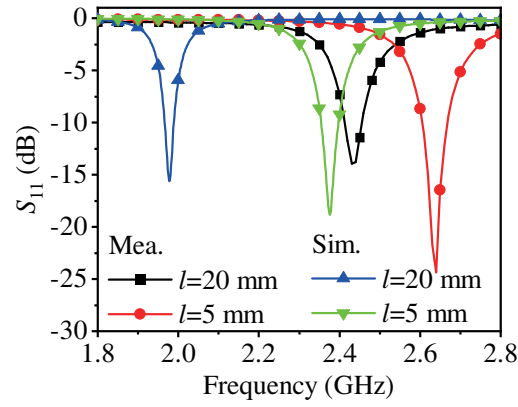
To verify the accuracy of the simulation results, the antenna samples with  $l = 5$  mm and  $l = 20$  mm were fabricated respectively. Figure 6 displays the photos of two fabricated antennas. The two layers of the antenna were bonded together using adhesive.

Figure 7 shows the measured results ( $S_{11}$ ) of the two antenna samples. The working frequencies of the two antennas are 2.64 GHz (Ant1) and 2.43 GHz (Ant2), respectively. While there were some differences between the measured and simulated results, their change trend remained consistent. The differences can be attributed to manufacturing precision and the relatively thick air gap  $g$  that exists between the upper and lower layers when the antenna is manually fabricated. As shown in the previous research results, when the value of  $g$  increases, the working frequency of the antenna increases correspondingly. Overall, the results confirm the feasibility of the proposed miniaturization method.

Figure 8 shows the simulated and measured results of the  $H$ -plane radiation pattern of the antennas at the working frequency. It shows that the measured and simulated results are basically consistent with each other.



**Figure 6.** Antenna samples.



**Figure 7.** Measured reflection coefficients of the fabricated antennas.

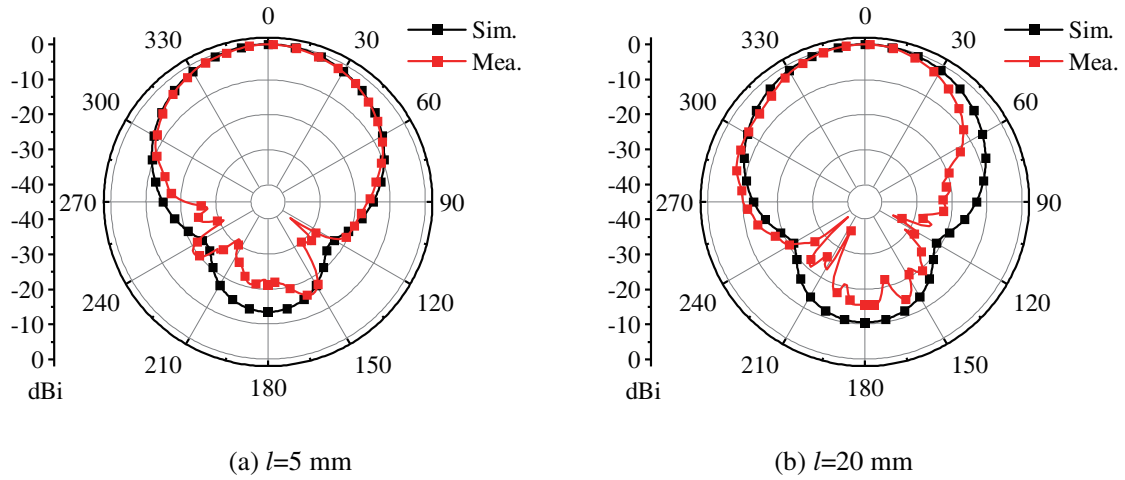


**Figure 8.** Simulated and measured  $H$ -plane radiation patterns of the proposed antenna at working frequency.

## 5. CONCLUSION

For a traditional rectangular patch antenna, its overall size can be reduced by inserting a middle metal strip layer. As the length of the metal strip is gradually increased, the working frequency of the antenna decreases correspondingly while the gain fluctuates within a small range. And the radiation pattern of the antenna remains basically unaffected. Combining this method with the decoupling method of the rectangular patch antenna, a smaller MIMO antenna could be designed. Furthermore, the proposed miniaturization method in this paper holds promising potential for implementation in the mobile and satellite communications.

## ACKNOWLEDGMENT

This work was supported by the National Natural Science Foundation of China (Grant No. 62161017), the Natural Science Foundation of Gansu Province of China (Grant No. 21JR7RA283), and the Young Schoars Science Foundation of Lanzhou Jiaotong University (Grant No. 1200061169 and No. 1520020821).

## REFERENCES

1. Zhao, A. B., J. Zhang, and G. Y. Tian, "Miniaturization of UHF RFID tag antenna sensors for corrosion characterization," *IEEE Sensors Journal*, Vol. 17, No. 23, 7908–7916, 2017.
2. So, K. K., H. Wong, K. M. Luk, and C. H. Chan, "Miniaturized circularly polarized patch antenna with low back radiation for GPS satellite communications," *IEEE Transactions on Antennas and Propagation*, Vol. 63, No. 12, 5934–5938, 2015.
3. Xu, L. J., Y. X. Guo, and W. Wu, "Miniaturized circularly polarized loop antenna for biomedical applications," *IEEE Transactions on Antennas and Propagation*, Vol. 63, No. 3, 922–930, 2015.
4. Juan, Y., W. C. Yang, and W. Q. Che, "Miniaturized low-profile circularly polarized metasurface antenna using capacitive loading," *IEEE Transactions on Antennas and Propagation*, Vol. 67, No. 5, 3527–3532, 2019.
5. Salih, A. A. and M. S. Sharawi, "A dual-band highly miniaturized patch antenna," *IEEE Antennas and Wireless Propagation Letters*, Vol. 15, 1783–1786, 2016.
6. Zhang, Y. D., C. R. Liu, X. G. Liu, K. Zhang, and X. M. Yang, "A wideband circularly polarized implantable antenna for 915 MHz ISM-band biotelemetry devices," *IEEE Antennas and Wireless Propagation Letters*, Vol. 17, No. 8, 1473–1477, 2018.
7. Huang, J. T., J. H. Shiao, and J. M. Wu, "A miniaturized Hilbert inverted-F antenna for wireless sensor network applications," *IEEE Transactions on Antennas and Propagation*, Vol. 58, No. 9, 3100–3103, 2010.
8. Amini, A., H. Oraizi, and M. A. Chaychi zadeh, "Miniaturized UWB log-periodic square fractal antenna," *IEEE Antennas and Wireless Propagation Letters*, Vol. 14, 1322–1325, 2015.
9. Fallahpour, M., M. T. Ghasr, and R. Zoughi, "Miniaturized reconfigurable multiband antenna for multiradio wireless communication," *IEEE Transactions on Antennas and Propagation*, Vol. 62, No. 12, 6049–6059, 2014.
10. Islam, M. M., M. T. Islam, and M. Samsuzzaman, M. R. I. Faruque, N. Misran, and M. F. Mansor, "A miniaturized antenna with negative index metamaterial based on modified SRR and CLS unit cell for UWB microwave imaging applications," *Materials*, Vol. 8, No. 2, 392–407, 2015.
11. Dave, T. P. and J. M. Rathod, "A thin-layer dielectric and metamaterial unit-cell stack loaded miniaturized SRR-based antenna for triple narrow band 4G-LTE applications," *International Journal of RF and Microwave Computer-Aided Engineering*, Vol. 29, No. 5, e21659, 2019.
12. Pedram, K., J. Nourinia, C. Ghobadi, N. Pouyanfar, and M. Karamirad, "Compact and miniaturized metamaterial-based microstrip fractal antenna with reconfigurable qualification," *International Journal of Electronics and Communications*, Vol. 114, 152959, 2020.

13. Lu, J. Y., H. C. Zhang, P. H. He, L. P. Zhang, and T. J. Cui, "Design of miniaturized antenna using corrugated microstrip," *IEEE Transactions on Antennas and Propagation*, Vol. 68, No. 3, 1918–1924, 2020.
14. Elijah, A. A. and M. Mokayef, "Miniature microstrip antenna for IoT application," *Materials Today: Proceedings*, Vol. 29, 43–47, 2020.
15. Farahbakhsh, A. and D. Zarifi, "Miniaturization of patch antennas by curved edges," *International Journal of Electronics and Communications*, Vol. 117, 153125, 2020.
16. Jahani, S., J. Rashed-Mohassel, and M. Shahabadi, "Miniaturization of circular patch antennas using MNG metamaterials," *IEEE Antennas and Wireless Propagation Letters*, Vol. 9, 1194–1196, 2010.
17. Farzami, F., K. Forooraghi, and M. Noroozariab, "Miniaturization of a microstrip antenna using a compact and thin magneto-dielectric substrate," *IEEE Antennas and Wireless Propagation Letters*, Vol. 10, 1540–1542, 2011.
18. Bakhtiari, A., R. A. Sadeghzadeh, and M. N. Moghadasi, "Gain enhanced miniaturized microstrip patch antenna using metamaterial superstrates," *IETE Journal of Research*, Vol. 65, No. 5, 635–640, 2019.
19. Li, M. J., K. M. Luk, L. Ge, and K. Zhang, "Miniaturization of magnetoelectric dipole antenna by using metamaterial loading," *IEEE Transactions on Antennas and Propagation*, Vol. 64, No. 11, 4914–4918, 2016.
20. Ouedraogo, R. O., E. J. Rothwell, K. Fuch, E. J. Rothwell, and A. R. Diaz, "Miniaturization of patch antennas using a metamaterial-inspired technique," *IEEE Transactions on Antennas and Propagation*, Vol. 60, No. 5, 2175–2182, 2012.
21. Adhiyoga, Y. G., S. F. Rahman, C. Apriono, and E. T. Rahardjo, "Miniaturized 5G antenna with enhanced gain by using stacked structure of split-ring resonator array and magneto-dielectric composite material," *IEEE Access*, Vol. 10, 35876–35887, 2022.
22. Chen, D. X., W. C. Yang, W. Q. Che, and Q. Xue, "Miniaturized wideband metasurface antennas using cross-layer capacitive loading," *IEEE Antennas and Wireless Propagation Letters*, Vol. 21, No. 1, 19–23, 2022.
23. Li, M., L. J. Jiang, and K. L. Yeung, "Novel and efficient parasitic decoupling network for closely coupled antennas," *IEEE Transactions on Antennas and Propagation*, Vol. 67, No. 6, 3574–3585, 2019.
24. Farahani, H. S., M. Veysi, M. Kamyab, and A. Tadjalli, "Mutual coupling reduction in patch antenna arrays using a UC-EBG superstrate," *IEEE Antennas and Wireless Propagation Letters*, Vol. 9, 57–59, 2010.
25. Ghosh, J., D. Mitra, and S. Das, "Mutual coupling reduction of slot antenna array by controlling surface wave propagation," *IEEE Transactions on Antennas and Propagation*, Vol. 67, No. 2, 1352–1357, 2019.
26. Wang, Y. and Z. W. Du, "A wideband printed dual-antenna system with a novel neutralization line for mobile terminals," *IEEE Antennas and Wireless Propagation Letters*, Vol. 12, 1428–1431, 2013.
27. Sun, L. B., Y. Li, and Z. J. Zhang, "Decoupling between extremely closely spaced patch antennas by mode cancellation method," *IEEE Transactions on Antennas and Propagation*, Vol. 69, No. 6, 3074–3083, 2021.
28. Zhou, W. Y., Z. L. Mei, M. Lu, and Y. B. Zhu, "Improved fully-connected neural network approach for decoupling microstrip antenna array design," *Journal of Electromagnetic Waves and Applications*, Vol. 36, No. 14, 1–14, 2022.